

Full Length Research Paper

Seismic refraction and resistivity imaging for assessment of groundwater seepage under a Dam site, Southwest of Saudi Arabia

Sayed S. R. Moustafa^{1*}, Elkhedr H. Ibrahim¹, Eslam Elawadi^{1,3}, Mohamed Metwaly^{1,2} and Naser Al Agami³

¹Department of Geology and Geophysics, Faculty of Science, King Saud University, Saudi Arabia.

²National Research Institute of Astronomy and Geophysics (NRIAG), Cairo, Egypt.

³Nuclear Materials Authority (NMA), Cairo, Egypt.

Accepted 8 October, 2012

Seismic refraction and resistivity imaging methods were used to investigate a Dam site in Southwest Saudi Arabia to delineate the source and pathway of groundwater seepage in the site. The selected methods have the possibility to give an image of the subsurface and map lateral and vertical variations in the subsurface geology of the site. For this purpose, 48-channels seismograph with geophone spacing of 5 m, near-offset distance of 10 m and a total far-offset distance which varies between 230 and 280 m was used. Three seismic lines were conducted and the acquired data were inverted to velocity sections using tomographic inversion. Velocity sections show that the subsurface is classified into four distinct seismic layers; starting with the topmost unconsolidated alluvium that is underlain by a second layer of saturated and/or compacted alluvium sediments. The third layer is associated with fractured basement, while the fourth layer is correlated to the hard massive bedrock with a relatively high velocity. These results indicate that the site is affected by faulting that resulted in two depressions which extends in the form of buried structural channels filled with porous alluvium and fractured greenstone. These depressions are considered zones of permeability and represent a favourable pathway for groundwater flow. These results and the zones of seepage are confirmed and verified using resistivity imaging, where a low resistivity zone of thickness up to 22 m is observed. This low resistivity zone is interpreted as a layer of alluvial sediment saturated with groundwater, which may indicate possible seepage flow.

Key words: Seismic refraction, resistivity imaging, site investigation, Saudi Arabia.

INTRODUCTION

The use of geophysical methods for investigating a site is increasingly becoming popular all over the world and has the possibility to give an image of the subsurface to the geologists and geotechnical engineers (Benson et al., 1984; Goldstein, 1994; Benson and Yuhr, 1995, 2002).

In this respect, seismic refraction is the most efficient geophysical tool used increasingly in site investigation for civil engineering. It is widely applied in investigating the shallow subsurface conditions in sites such as roads, tunnels, dams, quarries, hydroelectric power plants,

subways, nuclear power plants, bridges and many other purposes (Sjogren and Sandberg, 1979; Dutta, 1984; Kilty et al., 1986; Hatherly and Neville, 1986). Particularly, when used in conjunction with the exploratory drill, significant information about the subsurface layers in terms of velocities, thickness, and water saturation as well as elastic properties can be obtained. Moreover, geoelectric resistivity imaging has also been used in many studies in site investigation for civil engineering (Aizebeokhai, 2010; Yilmaz, 2011; Coşkun, 2012).

Field layout of refraction survey should be designed according to the site situation, required depth and resolution of subsurface investigation. However, increasing the efficiency of the source energy, stacking

*Corresponding author. E-mail: smoustafa@ksu.edu.sa.

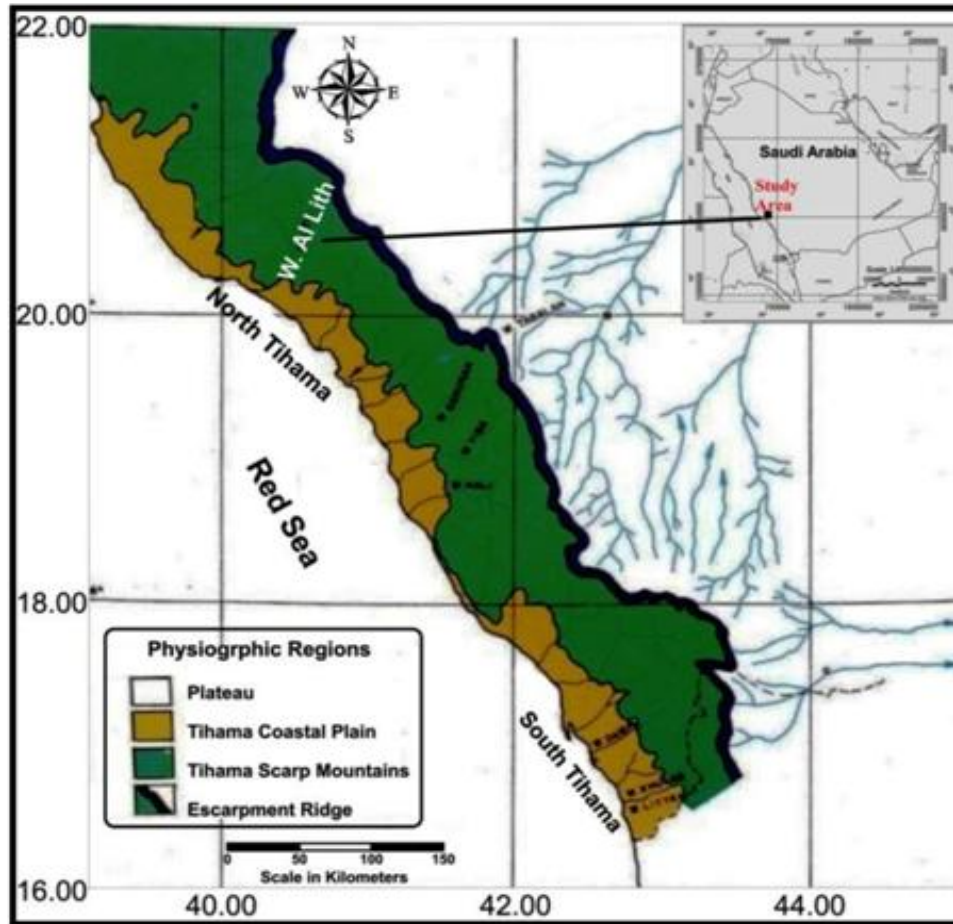


Figure 1. Location map of the investigated site.

and filtering of raw data improve the quality of refraction records. The basic field practices and methods of interpreting the data have not changed with time, although specialized interpretation techniques have been proposed and developed for some difficult cases. Foreknowledge of site conditions and understanding of its geological background always assist in resolving the raw data into meaningful information. In this study, resistivity imaging is also used in order to provide finer details about lateral and vertical variations in subsurface moisture, water content and near surface geology in the investigating site.

The reason behind conducting this research was the leakage or seepage of large quantity of groundwater beneath the proposed site of a Wadi Dam. In spite of grouting up to the depth of 1 m beneath the bedrock surface, huge amount of groundwater continued to flow. Therefore, the main objective of this survey is to investigate the shallow subsurface condition under the investigated site using seismic refraction and resistivity imaging survey in order to uncover the puzzle behind the source and pathway of the groundwater in the proposed site. The results will be of vital importance for engineering

evaluation of the Dam site.

METHODOLOGY

Location and brief geology

The study site is located in Al-Lith Basin that is situated in the Southwest of Saudi Arabia between latitudes $20^{\circ} 30' 30''$ and $20^{\circ} 30' 42''$ N and longitudes $40^{\circ} 28' 34''$ and $40^{\circ} 28' 43''$ E (Figure 1), draining from the Escarpment Ridge to the Red Sea with a catchment area of about 3079 km². The Al-Lith Basin is located on the western side of the Escarpment Ridge draining westerly to the Tihama Coastal Plains and subsequently to the Red Sea. High mountainous slopes of the escarpment decrease down to the flat alluvium Tihama Coastal Plain adjacent to the Red Sea. The change in basin relief has an overall elevation change of some 2750 m in a distance of approximately 150 km (Brown et al., 1963).

Previous geologic mapping of this region is described in the work of Brown et al. (1963), Wier and Hadley (1975), and Hadley and Fleck (1980). The geologic section at the proposed site starts with alluvium deposits that are typically flash flood deposits of ephemeral stream, composed of various size fragments ranging from silt to boulder size, and showing fining upward sequence, with boulder and pebbles at the base to sand and silt at the top. The Wadi alluvium was deposited on irregular surface, so the thickness

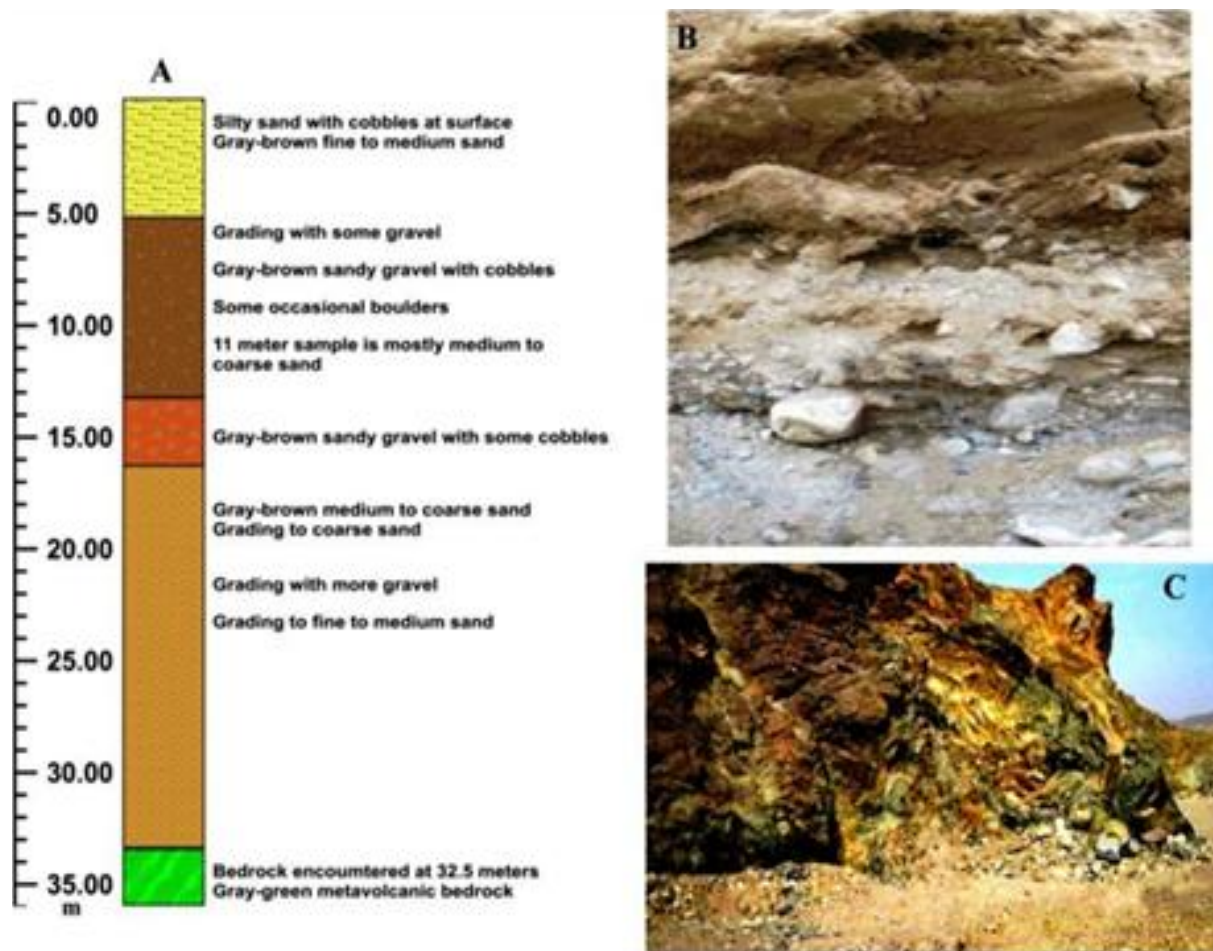


Figure 2. Lithologic column of a drilled borehole in the study area (A), photographic picture of the alluvium overburden (B) and Baish group (C).

of alluvium is highly variable-based on the paleotopography of the underlying rock units.

Near the border or periphery of the Wadi, the deposits are more coarser and represented by Wadi terrace deposits mainly of pebble size fragments, which is not easy to drill through it. While near the Wadi center, the deposits are mainly channel, fill sediments of sand size with subordinate gravels (Figure 2A and B). The central part of the Wadi is occupied by interbedded clay, silt, sand and gravel alluvium that have good storage and conductive properties and ranging in thickness from a few meters to more than 40 m.

Apart from recent Wadi infill alluvium, the alluvium deposits predominantly are underlain by highly fractured rock unit with thickness of this horizon ranges from 5 to 25 m. The interconnected fractures have a good permeability and allow the water to move through it. We must take in our consideration that the contact surface between the alluvium and the underlying fracture basement is a weakness plain and the water can move on this surface below the upper stream cofferdam, the second surface is between the fracture rocks and massive compact fresh rocks. The Baish group (Figure 2C) that is composed mainly of amphibolite, amphibolite schist, and quartz rich schist underlies this fractured rock unit. Generally, the rocks in this group have been metamorphosed to greenschist facies, which eventually gave rise to formation of greenstone and intruded by younger granitic rocks, which particularly crop out in the study area.

Data acquisition

The main purpose of this study is to investigate a Dam site in the Southwest of Saudi Arabia, using shallow seismic refraction and resistivity imaging methods in order to delineate the source and pathway of groundwater seepage in the site. Shallow seismic refraction and resistivity imaging have the possibility to give an image of the subsurface and map lateral and vertical variations in the subsurface geology of the site. In the following, brief accounts of the conducted data acquisition for employed methods are discussed.

Shallow seismic data acquisition

Seismic survey has been carried out along three lines around 250 to 280 m using 48-channel seismograph, with 5 m spacing and near-offset distance of 10 m (Figure 3).

The first line (A-A') was conducted along the cofferdam and the other two lines (B-B' and C-C') were parallel to it on the downstream side. Geophones with natural frequency around 40 Hz were used to provide adequate signals with usable frequency content. Using weight dropping, three shots were fired for every line. The first shot is a normal shot at a distance of 10 m before first geophone (G1) located at 0 m, the second shot is a central shot

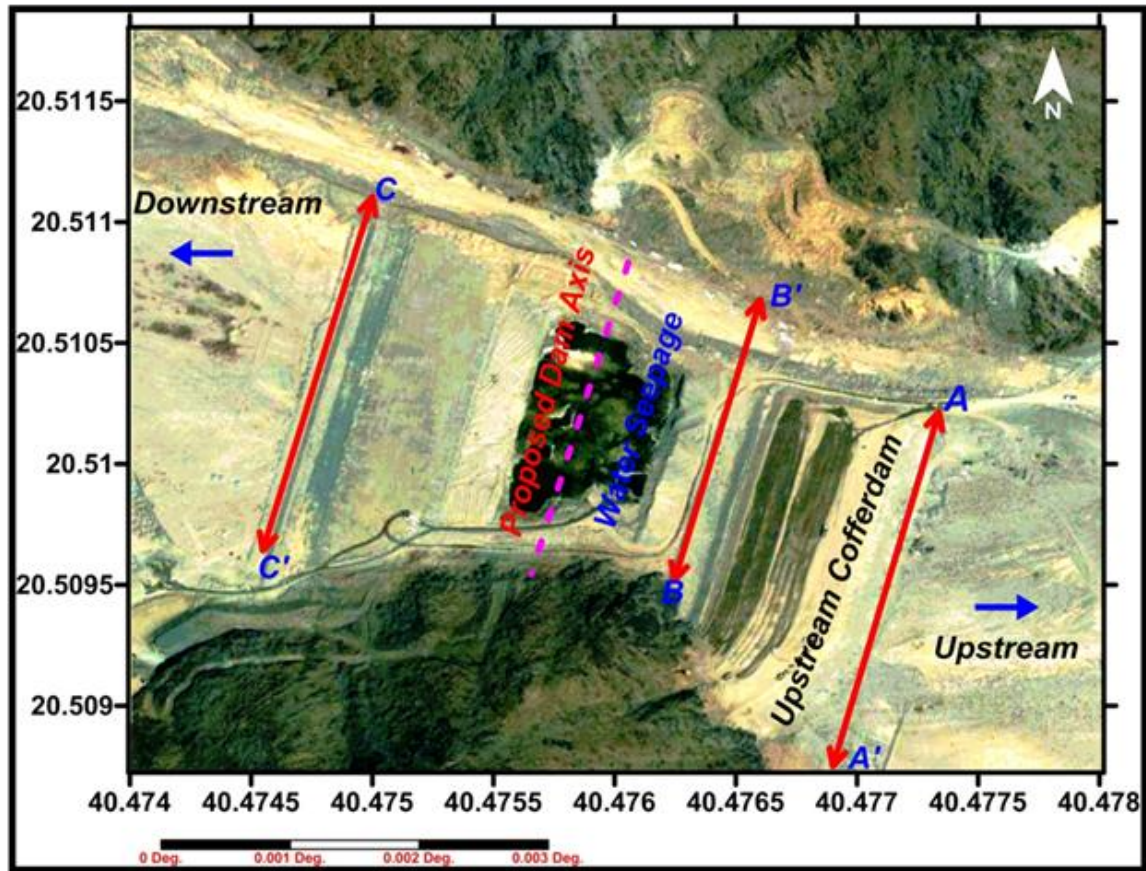


Figure 3. location map of the surveyed shallow seismic refraction lines. The geoelectric resistivity line coincides with the seismic line A-A'.

between the 24 and 25th geophones and the last shot is a reverse shot which was next to geophone 48. The elevations along the acquired seismic lines were taken using handheld global positioning systems (GPS) data that show no remarkable change in elevation that ranges from 197 to 200 m across the surveyed site, that is, the seismic lines nearly follow horizontal or near horizontal ground surfaces.

Resistivity data acquisition

Resistivity data are acquired along only one survey line that consists of three profiles, which is located in the upstream side of the cofferdam at the same location of line A-A' (Figure 3).

Collecting resistivity data near the other two seismic lines were not possible due to physiographic problems within the dam site where many fractured and weathered rocks cover the area resulted from engineering works done for preliminary preparation of dam's constructions.

Most of the electrical resistivity techniques require injection of electrical currents into the subsurface via a pair of electrodes planted on the ground. By measuring the resulting variations in electrical potential at other pairs of planted electrodes, it is possible to determine the variations in resistivity (Dobrin, 1988; Ozcep et al., 2009; Alile et al., 2011). For the current study, geoelectric data were acquired using the Schlumberger configuration, with electrode spacing of 10 m for Profiles 1 and 2 and 5 m for Profile 3. The *DMT GmbH* RESECS multi-electrode control system was used to acquire

these data. The RESECS multi-electrode control system is a PC controlled DC resistivity meter system for high-resolution research, tomography, and monitoring applications.

Data processing

The ultimate aim of the conducted seismic and geoelectric surveys is to determine the subsurface structure and resistivity distribution with depth on the basis of surface measurements of the p-wave seismic velocities and apparent resistivity and to interpret it in terms of geology or hydrogeology.

Seismic data processing

The recorded seismic data were uploaded to computer and processed using *SeisImager/2D™* system. The first arrival times were picked using the *Pickwin™* module and inversion of the travel time data were carried out in *Plotrefa™*. Arrival times versus shot point-to-geophone distance (Time-Distance curves) were plotted. The slopes of these time-distance segments are inversely proportional to the apparent velocity of seismic waves in that layer of the earth.

Two types of inversions, namely time-term inversion and, tomographic inversion, have been performed. To generate initial velocity model, the time-term inversion was firstly used. This inversion method assumes that the subsurface is vertically stratified

Table 1. Identification of subsurface rock layers.

Subsurface strata	Seismic velocity
Unconsolidated overburden	≈ 300 - 900
Compacted overburden	≈ 700 - 2000
Fractured greenstone	≈ 2000 - 3500
Hard and massive bedrock	≈ 3000 - 6000

without lateral changes in velocity. The depths to the top of the underlying layers are calculated under each point on the travel time versus offset distance plot. For obtaining the final results, tomographic inversion (Boschetti et al., 1996; Schuster and Quintus-Bosz, 1993; Sheehan et al., 2005; Wright, 2006; Zhang and Toksöz, 1998) was used. Such technique iteratively computes the travel time of the initial model using ray-tracing technique. The initial model obtained from the time-term inversion is modified to minimize the misfit between the computed travel time and the field data. The final model is obtained when the root-mean-square (rms) error converges such that further iterations would not reduce the rms error.

Geoelectric data processing

Generally, geoelectric data obtained during field measurements are classically presented as apparent resistivity pseudo-sections, which give an approximate picture of the subsurface resistivity.

Before the inversion process, separated profiles have been concatenated. Noise and spiky values were edited in order to obtain a true model representing continuous distribution of calculated electrical resistivity in the subsurface. Then inversion procedure was utilized using the least-squares method implemented in the rapid two-dimensional (2-D) resistivity *RES2DINV* inversion software (Loke and Barker, 1996). The inversion code is designed to interpolate and interpret field data of electrical geophysical prospecting (2-D sounding) of electrical resistivity (conductivity). It is based on the regularized least-squares optimization method involving finite-element and finite-difference methods (Sasaki, 1989; deGroot-Hedlin and Constable, 1990; Loke et al., 2003).

The optimization method was applied during the data inversion process, which is based on calculating the subsurface model close to the apparent resistivity one. Then the model is updated iteratively until a good matching between the calculated and measured sections was achieved.

RESULTS AND DISCUSSION

The measured p-wave velocities and apparent resistivity data are inverted to produce 2-D models of the subsurface using an iterative smoothness-constrained least squares inversion. In the following, interpretations of seismic refraction and resistivity imaging have the possibility to give an image of the subsurface and map lateral and vertical variations in the subsurface geology of the investigate dam site.

Seismic data interpretation

Shallow seismic refraction method gives information about the subsurface in terms of seismic velocities.

These velocities are directly related to the quality, hardness, compaction and water content of the medium. However, as qualitative classification, seismic velocity classification is used for identifying the subsurface rock layers in terms of unconsolidated or compacted sediments and fractured or hard bedrock (Table 1).

From the tomographic inversions, three refractors were detected for the seismic sections in the Dam site indicating presence of four distinct velocity layers; starting from the topmost low velocity layer to the high velocity layer of the hard massive bedrock. It is important to state that the relative thickness of the interpreted layers at different locations is interpreted with high confidence level. Meanwhile, the calculated thickness and velocities of the seismic layers are interpreted in light of the borehole and field investigation results. The data of the seismic sections gathered during the present survey along three seismic lines are also discussed.

Seismic line A-A'

This line is located on the upstream cofferdam with total length of 260 m. The travel time-distance curves and the corresponding 2-D ground model for this line are shown in Figure 4.

The results indicate that the subsurface structure consists of four seismic layers; the first layer is unsaturated overburden with seismic velocity range from 600 to 700 m/s and thickness varies from 3 to 48 m. The second layer is a saturated alluvium with velocity range from 700 to 2100 m/s and maximum thickness of about 61 m. The third layer is fractured greenstone with seismic velocity range from 2100 to 3200 m/s and maximum thickness of 55 m. The fourth layer is massive greenstone with seismic velocity which exceeds 3200 m/s.

The interpreted subsurface model for this line shows deeper massive rock centered at distances of 42 and 167 m from the shot point. These two low velocity/depression zones indicate the existence of multiple shear zones cutting the massive bedrock, filled with alluvium deposits, and fractured greenstone bedrock that might associate with faulting affecting the Wadi site.

Seismic Line B-B'

This line is located in the western side of the upstream cofferdam with total length of 230 m (Figure 3). The travel time-distance curves and the corresponding 2-D ground model for this line are shown in Figure 5.

The obtained subsurface structure consists of four layers; the first layer is unsaturated overburden with seismic velocity ranges from 500 to 900 m/s and thickness which reaches 13 m. The seismic velocity of the second layer ranges from 900 to 2100 m/s, indicating a compact saturated alluvium. The thickness of this layer

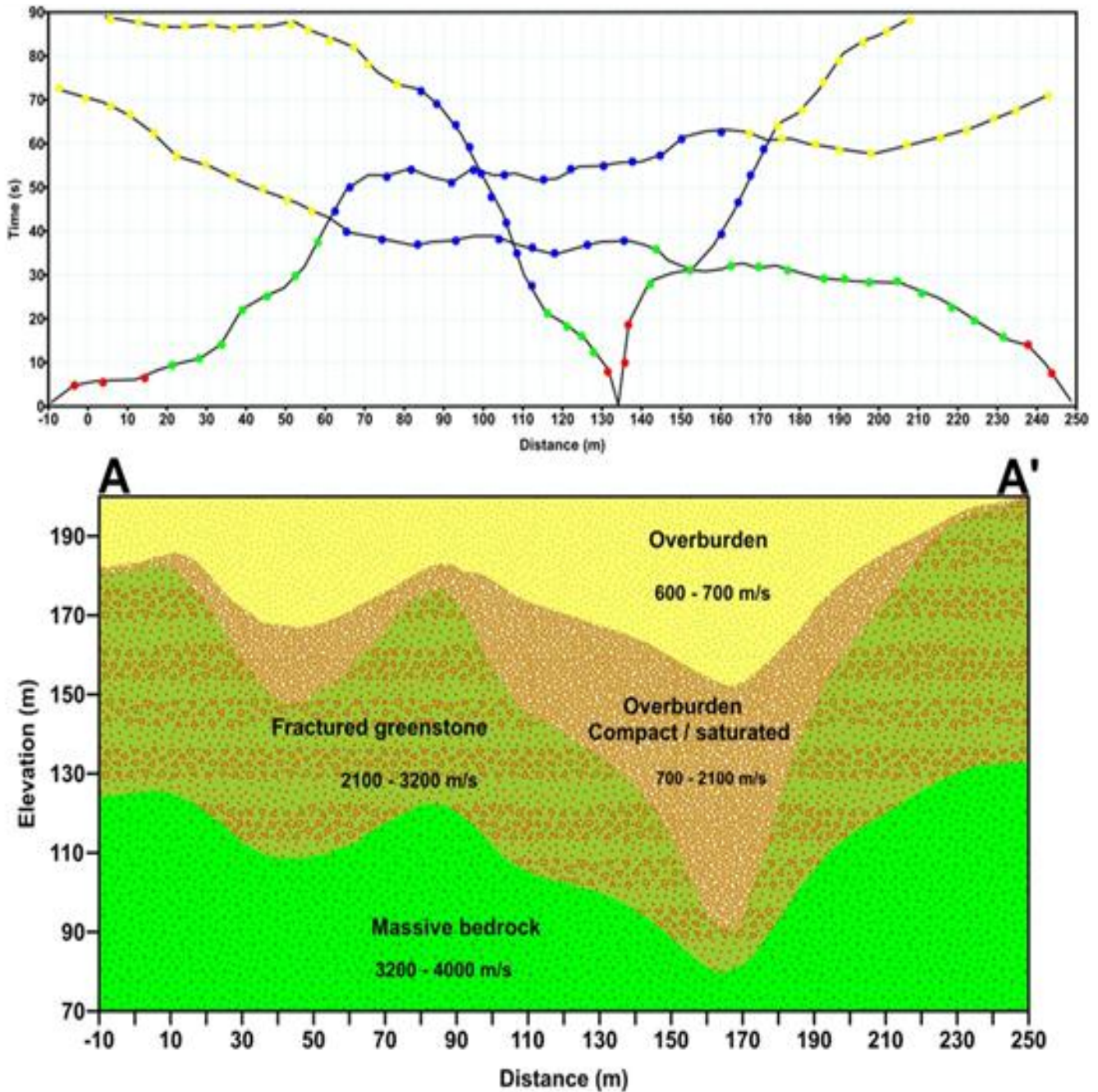


Figure 4. Travel time-distance curves (above) and the corresponding interpreted seismic cross section (below) across the seismic line A-A'.

along the seismic line varies from 8 to 66 m. Seismic velocities ranging from 2100 to 2900 m/s, suggest fractured saturated greenstone with thickness which reaches 50 m, characterize the third layer. Hard and massive bedrock is mapped below this layer with seismic velocities which exceeds 2900 m/s.

The interpreted subsurface model for this line shows deeper massive rock centered at distance of 30 and 146 m from the beginning of the line, indicating two structural

depressions filled with alluvium deposits and fractured greenstone.

Seismic Line C-C'

This line is located to the west of the downstream cofferdam with total length of 280 m. The travel time-distance curves and the corresponding 2-D ground model

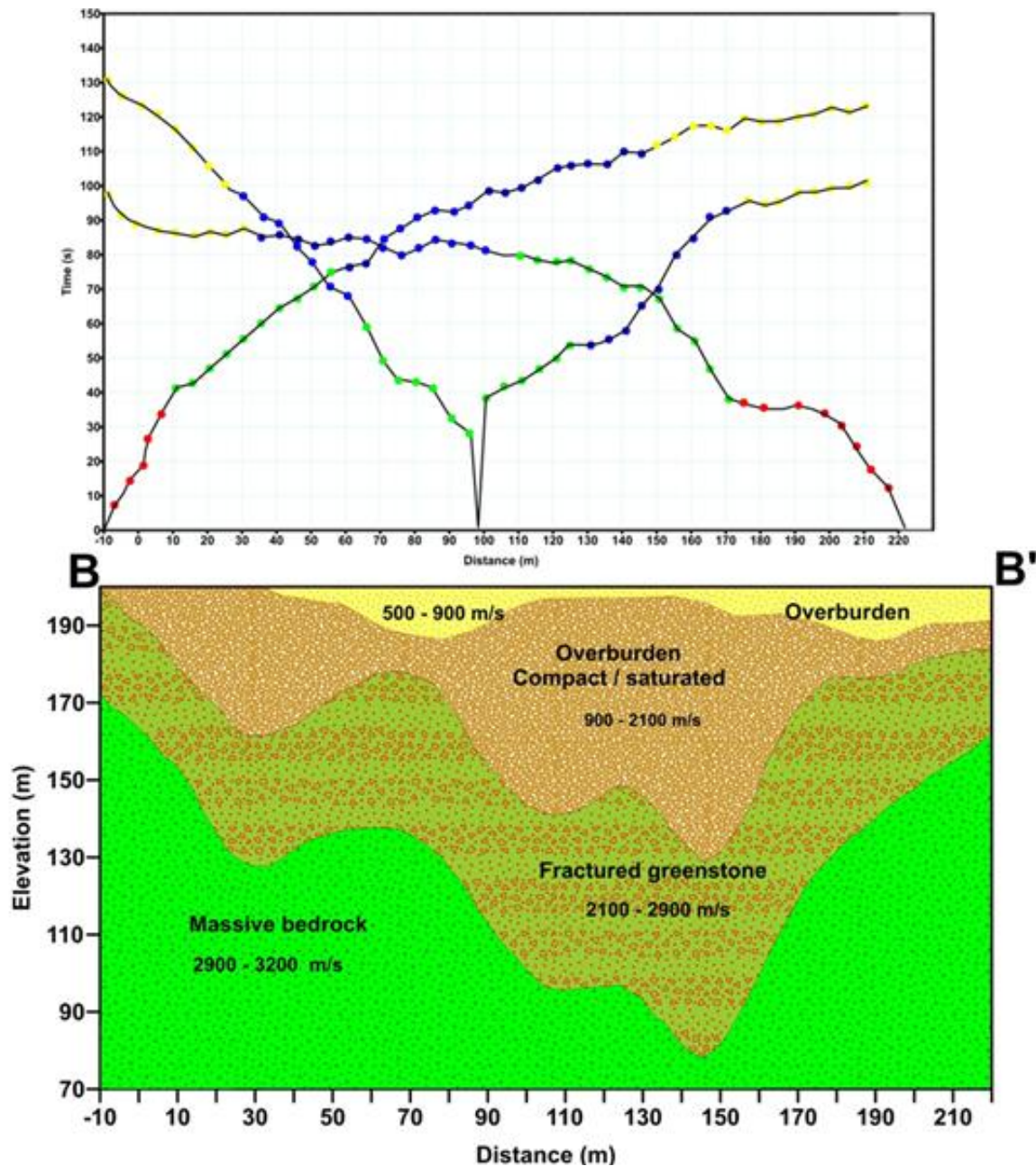


Figure 5. Travel time-distance curves (above) and the corresponding interpreted seismic cross section (below) across the seismic line B-B'.

of this line are shown in Figure 6.

The resulted 2-D ground model indicate that the first layer is manmade landfill and loose alluvium with seismic velocity ranges from 300 to 870 m/s and maximum thickness of about 27 m. Below this layer, the seismic velocities range from 870 to 1620 m/s, indicating a layer of a compact alluvium layer having a maximum thickness of 70 m. The third layer is characterized by seismic velocities ranging from 1620 to 3800 m/s, which is lower than the similar layers in the other two lines (A-A' and B-

B'), suggesting fractured greenstone. Hard and massive bedrock is mapped below this layer with seismic velocities which exceeds 3800 m/s.

The interpreted ground model along seismic line D-D' indicates deeper basement centered at distances of 91 and 197 m from the shot point. Such two deeper basement zones are interpreted as low velocity structural depressions indicating the existence of shear zones filled with alluvium deposits, and fractured greenstone bedrock cutting the massive bedrock that might associate faulting

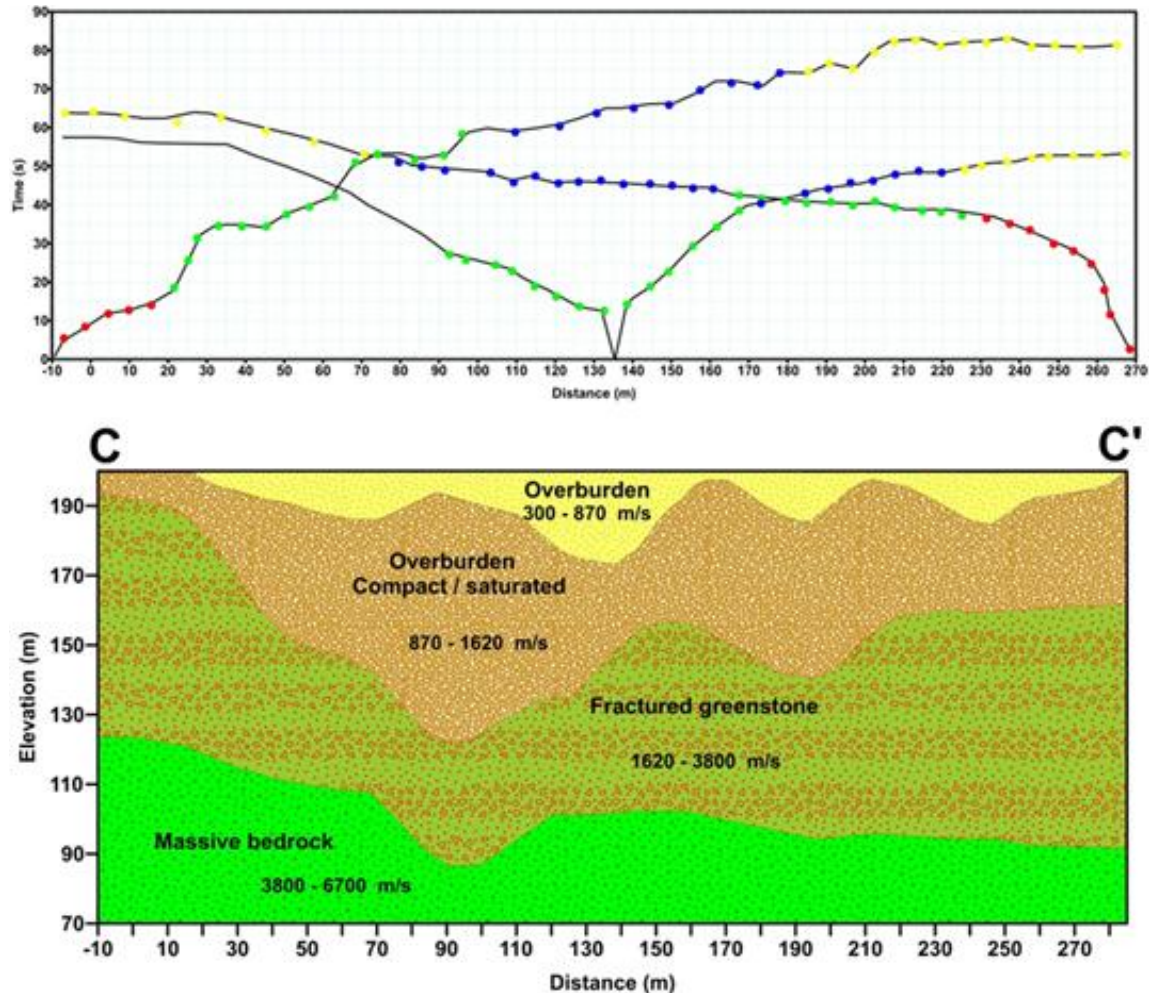


Figure 6. Travel time-distance curves (above) and the corresponding interpreted seismic cross section (below) across the seismic line C-C'.

affected the Dam site.

Resistivity data interpretation

2-D resistivity Imaging was conducted along one survey line that consists of two successive profiles. Inverted resistivity sections of the two profiles are merged as one line to facilitate interpretation. The two measured resistivity profiles are located to the eastern side of the upstream cofferdam. The resulted merged profile extends in the north-south direction on the same location and trend of the first seismic profile (A-A') to cover the width of the upstream Wadi (Figure 3).

Generally, the resistivity profiles start with a thin high resistivity layer with depth range of about 2 m with resistivity exceeds of 1000 Ohm.m (Figure 7). This layer is correlated to unsaturated loose sediments that represent the aeration zone in the site. This topmost layer is underlain by a lower resistivity layer of 30 to 200

Ohm.m and variable thickness up to an average depth of 22 m. This low resistivity layer is related to the water saturated alluvium deposits.

The estimated low resistivity values are due to the presence of higher groundwater content of the alluvium sediment layer, which indicates possible seepage flow. These seepage locations are also verified using the seismic refraction data. The southern side of the geoelectric section is characterized by the presence of a relatively high resistive zone with resistivity exceeds of 1000 ohm.m that is interpreted as a grouting cement injected into the ground in order to prevent the groundwater flow. It is important to mention that the resolution of these two profiles (10 m electrode spacing) does not get to the compact basement and the maximum depth is about 25 m.

The results of refraction survey have shown that the main Wadi channel is sub-divided into two main depressions filled with alluvium and fractured greenstone and linked by narrow sharp uplifted wall. It appears that

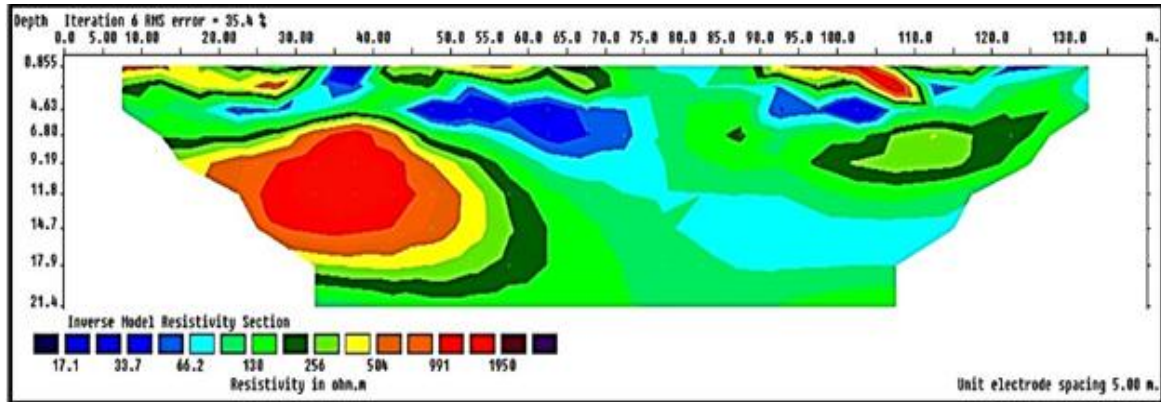


Figure 7. Geoelectric resistivity 2-D section across the survey line A-A'.

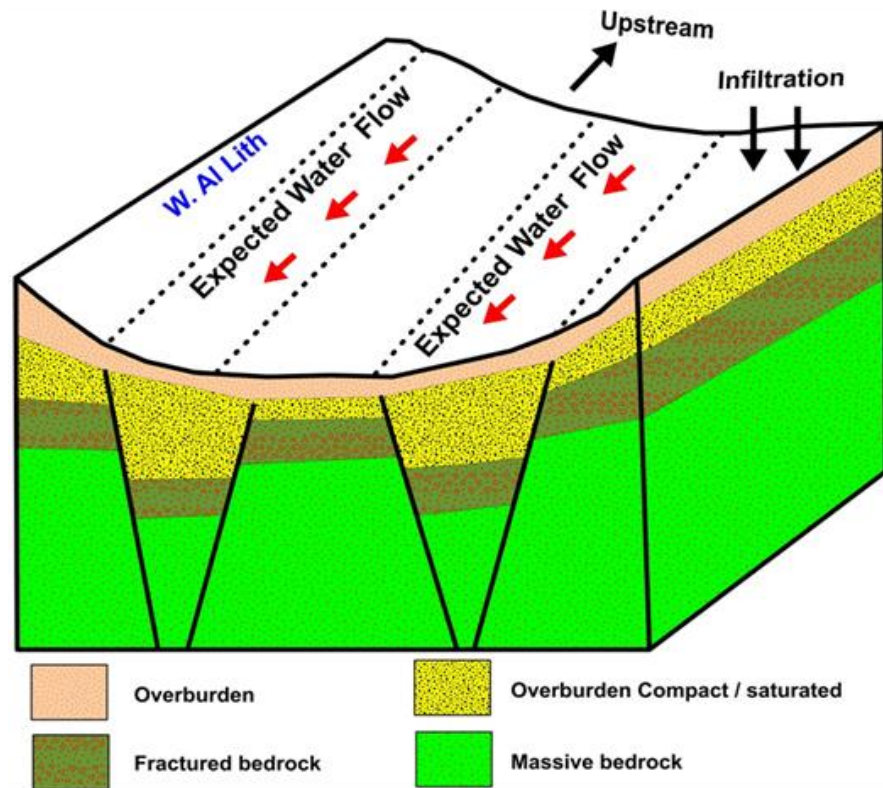


Figure 8. Schematic diagram showing the buried faulted channels crossing the site and the flow of the groundwater.

these depressions extend in the site resembling buried structural channels crossing the site (Figure 8). These results and the zones of seepage are confirmed and verified using resistivity imaging, where a low resistivity zone of thickness up to 22 m is observed. This low resistivity zone is interpreted as a layer of alluvial sediment saturated with groundwater, which may indicate possible seepage flow.

The expected flow of the groundwater through these

interpreted structural channels is based on the porous alluvium deposits and fractured greenstone that filled these channels and the faults that bounded these channels. The combination of the faults and thick alluvium and fractured greenstone section are considered zones of permeability and have higher transmissivity values than the surrounding massive bedrock, therefore, represent a particularly favourable conduit or pathway for groundwater flow. This geologic situation makes these

channels good pathways for groundwater to the site and the amount of water that reaches the Wadi from overland areas of Al-Lith Basin fed this groundwater flow and recharges the downstream depressions. The spatial relationship between traced structural channel (depression) and the location of surface groundwater seepage in combination of the field lithological and hydrogeological information confirmed the success of the seismic survey to locate the source and direction of the water seepage in the investigated site.

Conclusions

Refraction seismic surveys were conducted at Al-Lith Dam site to investigate the shallow subsurface and determine the depth to the fractured and compact basement at the area as well as mapping any geologic structure that might be responsible for water leakage beneath the upstream cofferdam.

The acquired data were inverted to velocity sections using the tomographic inversion method. The inverted velocity sections show that the shallow subsurface of the area is dominated by four seismic layers with distinct velocity level. The lower velocity layer (up to 900 m/s) corresponds to the unsaturated alluvium layer and filling materials cover most of the area. The second layer with intermediate velocity (from 700 to 2000 m/s) is related to the saturated alluvium, while the third layer with a relatively high velocity (from 2000 to 3500 m/s) is associated with fractured basement. The fourth layer with seismic velocity exceeds of 3500 m/s is correlated to the hard and massive bedrock. These four layers could be interpreted almost in all lines with variable depths and thickness. The results of refraction survey have shown that the main Wadi channel is sub-divided into two main depressions filled with alluvium and fractured greenstone and linked by narrow sharp uplifted wall. It appears that these depressions extend in the site resembling buried structural channels crossing the site. These results and the zones of seepage are confirmed and verified using resistivity imaging

ACKNOWLEDGEMENTS

This work was supported financially by the Research Centre, College of Science, King Saud University, Saudi Arabia.

REFERENCES

- Aizebeokhai AP (2010). 2D and 3D geoelectrical resistivity imaging: Theory and field design. *Sci. Res. Essays* 5(23):3592-3605.
- Alile OM, Ujuanbi O, Evbuomwan IA (2011). Geoelectric investigation of groundwater in Obaretin -Iyanomon locality, Edo state, Nigeria. *J. G. Min. Res.* 3(1):13-20.
- Benson RC, Glaccum R, Noel M (1984). Geophysical techniques for sensing buried wastes and waste migration. NTIS PB84-198449.
- Benson RC, Yuhr L (1995). Geophysical methods for environmental assessment. *Geoenvironmental 2000, ASCE Conf. Exhib., New Orleans.*
- Benson RC, Yuhr L (2002). Site characterization strategies: old and new. Second Annual Conference on the Application of Geophysical and NDT Methodologies to Transportation Facilities, Federal Highway Administration, April 15-19, Los Angeles, California.
- Brown GF, Jackson RO, Bogue RG, MacLean WH (1963). Geologic map of the southern Hijaz quadrangle, Kingdom of Saudi Arabia: U.S. Geological Survey Miscellaneous Geologic Investigations Map 1-210-A, scale 1:500,000.
- Boschetti F, Dentith MC, List RD (1996). Inversion of seismic refraction data using genetic algorithms. *Geophysics* 61:1715-1727.
- Coşkun N (2012). The effectiveness of electrical resistivity imaging in sinkhole investigations. *Int. J. Phys. Sci.* 7(15):2398-2405.
- deGroot-Hedlin C, Constable S (1990). Occam's inversion to generate smooth two-dimensional models from magnetotelluric data. *Geophys.* 55:1613-1624.
- Dobrin MB (1988). *Introduction to Geophysical Prospecting.* New York: McGraw-Hill. P. 867.
- Dutta NP (1984). Seismic refraction method to study the foundation rock of a Dam. *Geophys. Prospect* 32:1103-1110.
- Goldstein NE (1994). Expedited site characterization geophysics: Geophysical methods and tools for site characterization. Prepared for the U.S. Department of Energy by Lawrence Berkeley Laboratory, Univ. of California. 124 p.
- Hadley DG, Fleck RJ (1980). Reconnaissance geologic map of the Al-Lith quadrangle, sheet 20/40 C, Kingdom of Saudi Arabia: Saudi Arabian Directorate General of Mineral Resources Geologic Map GM-32, 10 p., 1 sheet, scale 1:100,000.
- Hatherly PJ, Neville MJ (1986). Experience with the generalized reciprocal method of seismic refraction interpretation for shallow seismic engineering site investigation. *Geophysics* 51:276-288
- Kilty KT, Noriss RA, McLamore WR, Hennon KP, Euge K (1986). Seismic refraction at Horse Dam. An application of the generalized reciprocal method. *Geophysics* 51:266-272.
- Loke MH, Barker RD (1996). Practical techniques for 3-D resistivity surveys and data inversion. *Geophysics* 44:499-523.
- Loke MH, Acworth I, Dahlin T (2003). A comparison of smooth and blocky inversion methods in 2-D electric imaging surveys. *Explor. Geophys.* 34:182-187.
- Ozcep F, Tezel O, Asci M (2009). Correlation between electrical resistivity and soil-water content: Istanbul and Golcuk. *Int. J. Phys. Sci.* (4)6:362-365.
- Sasaki Y (1989). Two-dimensional joint inversion of magnetotelluric and dipole-dipole resistivity data. *Geophysics* 54:174-187.
- Schuster GT, Quintus-Bosz A (1993). Wavepath eikonal travel time inversion. *Geophysics* 58:1314-1323.
- Sheehan JR, Doll WE, Mandell WA (2005). An evaluation of methods and available software for seismic refraction tomography analysis. *J. Environ. Eng. Geophys.* 10:21-34.
- Sjogren BO, Sandberg J (1979). Seismic classification of rock mass qualities. *Geophys. Prospect* 27:409-442.
- Wier KL, Hadley DG (1975). Reconnaissance geology of the Wadi Sa'diyah quadrangle, sheet 20/40 A, Kingdom of Saudi Arabia: U.S. Geological Survey Open-File Report 75-493, 27 p., scale 1:100,000.
- Wright C (2006). The LSDARC method of refraction analysis: principles, practical considerations and advantages. *Near Surface Geophysics* 4:189-202.
- Yilmaz Y (2011). A case study of the application of electrical resistivity imaging for investigation of a landslide along highway. *Int. J. Phys. Sci.* 6(24):5843-5849.
- Zhang J, Toksöz MN (1998). Nonlinear refraction travel time tomography. *Geophysics* 63:1726-1737.